Home

# THE EFFECT OF SPATIAL COREELATIONS ON THE PERFORMANCE OF 2-D RAKE RECEIVERS IN BAD URBAN CHANNELS

Asrar U. H. Sheikh and Saad Muhammed Al-Ahmadi
Department of Electrical Engineering
King Fahad University of Petroleum & Minerals
KFUPM Box 5038, Dhahran 31261, Saudi Arabia.
asrarhaq@kfupm.edu.sa

## Abstract

**The wideband elliptical model is used for bad urban channels. The clustered scatterers are assumed to have bi-variate Gaussian distributions. Propagation models are used to derive AOA distributions are derived. The resulting spatial correlations are computed. The effect of these correlations on the performance of 2-D Rake receivers is investigated analytically and by simulations for different antenna spacing and channel power delay profiles.**

## I. INTRODUCTION

The need for larger user capacity and higher data rates services in wireless communications has initiated the trend towards the use of antenna arrays (as in 2-D RAKE receivers) [1]. However, the spatial diversity gain of such receivers is strongly affected by the spatial correlations at the antenna array elements. The spatial correlation is dependent on the Angle of Arrival (AoA) statistics and the mean angle of arrival. In [2], a raised cosine distribution for the AoA's was used to compute the spatial correlations at the BS for both the broadside and end fire cases. In [3], the AoA's were assumed to be uniformly distributed over the angular range [-Ä, Ä] and the spatial correlations were computed for different values of Ä. In this paper, a three-path wideband elliptical model for bad urban Nakagami faded channels is introduced with the appropriate scatterers distributions, Then, this geometrically-based model is used to derive the AoA distribution and compute the spatial correlation matrix for each path are computed.

## II. CHANNEL MODEL

### *A. Channel Geometry and Scatterers Distributions.*

The proposed channel geometry for bad urban channels is shown in Fig. 1. In this model, the scatterers are assumed to be characterized by the existence of a mixture of open areas and densely built-up zones with a large variety of different building heights. The equivalent model of the scattering and propagation mechanisms in a bad urban environment has a geometry that is similar to the wideband elliptical model, each path is assumed to be due to a cluster of scatterers, which lie within the first ellipse or in between the concentric ellipses with foci at the BS and the MS, respectively.

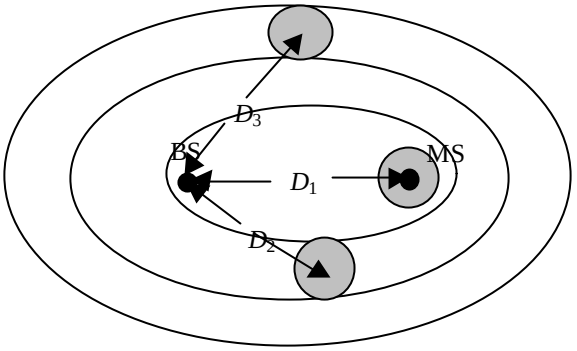


Figure 1 A geometrical model of BU channels.

The scatterers around the MS (with a radius $R_1$) generate the first arriving multi-path component at the BS receiver; the second cluster of scatterers (within the second ellipse and with a radius $R_2$) generates the second path and so on for the other paths. In the context here, a three-path model is considered. Clearly, this model can be extended to any number of paths. The scatterer's probability density functions (pdf's), assuming that the scatterers (in the three clusters) have the (bi-variate Gaussian) distribution, can be expressed as,

$$p(r_b,\theta) = \frac{r_b}{2\pi\sigma_i^{\,2}} \cdot \exp\left[-\frac{r_b^{\,2} - 2r_b D_i \cos\theta + D_i^{\,2}}{2\sigma_i^{\,2}}\right] \qquad (1)$$

$$i = 1,2,3.$$

where $r_b$ denotes the distance as measured from the BS to a scatterer 'S' and $\sigma$ is the variance of the cluster's scatterers and is an environment dependent parameter, $D_2$ and $D_3$ denote the distances between the BS and the centers of the clusters as shown in Fig. 1. The distances $D_2$ and $D_3$ can be calculated for the set of the mean AoA's ($\phi_2$ and $\phi_3$) using the equations of the ellipses that correspond to the average delay of each path as

$$D_2 = \frac{4a_2^{\,2} - D_1^{\,2}}{4a_2 - 2D_1\cos\phi_2} \qquad (2)$$

$$D_3 = \frac{4a_3^{\,2} - D_1^{\,2}}{4a_3 - 2D_1\cos\phi_3} \qquad (3)$$

where $a_2$ and $a_3$ are given as

$$a_2 = \frac{D_1}{2} + R_1 + R_2 \quad (4)$$

$$a_3 = \frac{D_1}{2} + R_1 + 2R_2 + R_3 \quad (5)$$

*B. Angle of Arrival Statistics*

The AoA statistics of the first path in LOS BU micro-cells can be modeled using the concept of mixed distributions, where the pdf can be expressed as the sum of two parameterized pdf's

$$p(\theta) = (1-\sqrt{1-m^{-1}}) \cdot p_d(\theta) + \sqrt{1-m^{-1}} \cdot \delta(\theta - \theta_{LOS}) \quad , -\pi \le \theta \le \pi, \quad m \ge 1 \quad (6)$$

where $m$ is the Nakagami fading parameter and $\theta_{LOS}$ is the AoA of the LOS component. The term $p_d(\theta)$ stands for the pdf of the diffused component The AoA pdf of the other multi-path components can be determined using the following modified pdf

$$p(\theta) = (1-\sqrt{1-m^{-1}}) \cdot p_d(\theta) + \sqrt{1-m^{-1}} \cdot \delta(\theta - \theta_{SPC}) \quad (7)$$

where $\theta_{SPC}$ denotes the AoA of a possibly a specular component contained in that path.

It has been shown in [4] that the AoA pdfs of the diffused components of the three paths are given as in (8) where

$$p(\theta) = \frac{1}{2\sqrt{2\pi}\,\sigma_i} . D_i \cos\theta . \exp\left[\frac{D_i^2(\cos^2\theta - 1)}{2\sigma_i^2}\right] \cdot \left[ erf\left(\frac{bb_i - D_i\cos\theta}{\sqrt{2}\sigma_i}\right) + erf\left(\frac{aa_i - D_i\cos\theta}{\sqrt{2}\sigma_i}\right)\right] + \left(\frac{1}{2\pi}\right) \cdot \exp\left(\frac{-D_i^2}{2\sigma_i^2}\right) \cdot \left\{ \exp\left[\frac{-aa_i(aa_i - 2D_i\cos\theta)}{2\sigma_i^2}\right] - \exp\left[\frac{-bb_i(bb_i - 2D_i\cos\theta)}{2\sigma_i^2}\right]\right\}, |\theta| \le \beta_i \quad (8)$$

$$, i = 1, 2, 3.$$

$$aa_i(\theta) = D_i\cos\theta - \sqrt{D_i^2\cos^2\theta - D_i^2 + R_i^2} \quad (9)$$

$$bb_i(\theta) = D_i\cos\theta + \sqrt{D_i^2\cos^2\theta - D_i^2 + R_i^2} \quad (10)$$

and

$$\beta_i = \sin^{-1}\left(\frac{R_i}{D_i}\right) \quad , i = 1, 2, 3. \quad (11)$$

The values parameters $R_1$, $R_2$, and $R_3$ can be determined from the geometry in Fig. 1. The values of the radii are determined by the resolution of the W-CDMA channel ($t$ 1/$W$). For example, the resulting path resolution for a 3.844 MHz transmission rate is 260 ìs. Thus, if the first path arrives with an average delay of $t_0$, the second path is expected to arrive with an average delay of $t_0$+260 ìs, which corresponds to a path length difference of 78 meters. Furthermore, the difference between the second and third ellipses will be 78 meters and hence the radii of the circles. Fig. 2 shows the plots of the pdf‘s of the AoA’s of the three paths. Clearly, BU environments do generate multi-paths in both the spatial and temporal domains. Wideband impulse response measurements in such environments in [5] have recorded the occurrence of strong peaks in the impulse responses, which are due to the separate clusters of scatterers.

*C. Spatial Correlations*

One of the main concerns in the analysis of the performance of antenna arrays systems in multi-path fading channels is the spatial correlation between the signals received at the *i*th and the *k*th antenna elements. The spatial correlation is defined as a measure of the correlation between the amplitudes of multi-path components that arrive with the same excess delay at the ULA (uniform linear array). Using the geometrical model of an ULA, with element spacing, $d$, and mean of direction of arrival, $\theta_0$, the normalized spatial correlation coefficient between a multi-path component received at the element “$k$” and its replica at the element “$l$” can be expressed as [3].

$$R = \left(|R_{xx}|^2 + |R_{xy}|^2\right)^{1/2} \quad (12)$$

where $R_{xx}$ and $R_{xy}$ denote the spatial correlations among real and imaginary components of the faded signals (at elements $k$ and $l$). Using a similar procedure to the one given in [3], $R_{xx}$ and $R_{xy}$ can be computed. The plots of the envelope spatial correlation coefficients of the signals corresponding to the first path, the second path and third paths are shown in Fig. 3 for different values of the standard deviation of the clustered scatterers. The results show that the paths are highly correlated due the small spread (variance) of scatterers ($\sigma_1$=30 m, $\sigma_2$=20 m and $\sigma_3$=15 m).

## III. BER ANALYSIS

*A. PDF of the signal to interference ratio (SINR)*

The SINR at the output of a 2-D RAKE receiver, that performs maximal ratio combining in both time and space, can be expressed as [6]

$$\gamma_s = \sum_{l=1}^{L} \gamma_l = \sum_{l=1}^{L}\sum_{i=1}^{M} \gamma_{l,i} \quad (13)$$

where $L$ denotes the number of the 2-RAKE temporal fingers and $M$ is the number of antenna array elements, $\gamma_{l,i}$ are the instantaneous SINR on the $l$th RAKE branch and on the $i$th array element, respectively. In Nakagami fading environments, using the reasonable assumption of $m_{l,1}$= …= $m_{l,M}$ =$m_l$ and $\Omega_{l,1}$=...,...= $\Omega_{l,,M}$ =$\Omega_l$, since the same path is received instantaneously at all the ULA elements,

Top

each $\gamma_{l,i}$ is gamma-distributed random variable with a pdf

$$p_{\gamma_{l,i}}(\gamma) = \left(\frac{m_l}{\overline{\Gamma}_l}\right) \cdot \frac{\gamma^{m_l - 1}}{\Gamma(m_l)} \cdot \exp\left(-\frac{m_l}{\overline{\Gamma}_l} \cdot \gamma\right) \tag{14}$$

where $\overline{\Gamma}_l$ is the average received SINR of the $l$th path. Putting $\Ë_l = \overline{\Gamma}_l / m_l$, the characteristic function of $\gamma_l$ is given as [7]

$$\Phi_l(t) = \left| I - j\Lambda_l t \hat{R}_s^{\,l} \right| = \prod_{i=1}^{M} (1 - j\Lambda_l \lambda_{l,i} t)^{-m_l} \tag{15}$$

where $I$ is $M \times M$ identity matrix and $\hat{R}_s^{\,l}$ is the normalized spatial correlation matrix of the signals received at the $l$th RAKE branch and $\lambda_{l,i}$ are the eigenvalues of $\hat{R}_s^{\,l}$ [3]. If there is no correlation between the faded signals in the diversity branches, then the eigenvalues must be equal to o unity. For correlated branches, (15) indicates that $\gamma_l$ has the same distribution as a linear combination of independent and identically distributed gamma variables as [6]

$$\gamma_l = \sum_{i=1}^{M} \lambda_{l,i} \gamma_{l,i} \tag{16}$$

Now the distribution of $\gamma_l$ can be approximated to a gamma distribution with the first two moments identical to those of the exact distribution of $\gamma_l$. Thus, the two parameters $\overline{\Gamma}_l^{\,d}$ and $m_l^{\,d}$ can be derived, respectively, as [6]

$$\overline{\Gamma}_l^{\,d} = \overline{\Gamma}_l \cdot \sum_{i=1}^{M} \lambda_{l,i} \tag{17}$$

and

$$m_l^{\,d} = \frac{\left(\sum_{i=1}^{M} \lambda_i\right)^2}{\sum_{i=1}^{M} \lambda_i^{\,2}} \cdot m_l \tag{18}$$

The distribution of $\gamma_s$, assuming that the 2-D RAKE temporal branches are uncorrelated, using results in [8], can be expressed as

$$p_{\gamma_s}(\gamma) = \frac{1}{\pi} \int_0^{\infty} \frac{\cos\left[\sum_{i=1}^{L} m_l^{\,d} \cdot \tan^{-1}\left(\frac{t}{\eta}\right) - t\gamma\right]}{\prod_{l=1}^{L}\left[1 + \left(\frac{t}{\eta}\right)\right]^{\frac{m_l^{\,d}}{2}}} dt \tag{19}$$

where $\eta = \dfrac{m_l^{\,d}}{\overline{\Gamma}_l^{\,d}}$ (20)

*B. Average Probability of Error*

The average probability of error is calculated from the conditional BER by averaging $P_e(\tilde{a}_s)$ over the pdf of $\tilde{a}_s$. So, using the alternative form of the conditional BER

$$P_e(s) = \frac{1}{2} \cdot erfc\left(\sqrt{\gamma_s}\right) = \frac{1}{2} \cdot erfc\left(\sqrt{\sigma_0 s}\right) \tag{21}$$

where $s$ is the random component of the SINR [9]

$$s = \frac{1}{\Omega_0} \cdot \sum_{n=1}^{L_r} \{a_n^{(1)}\}^2 \tag{22}$$

where $\Omega_0$ is the average power of the first path and $\{a_n\}$ is the path coefficient, and $\sigma_0$ is the deterministic component is given as

$$\sigma_0 = \left\{ \frac{2 \cdot (K-1) \cdot q(L,\delta)}{3N} + \frac{q(L,\delta) - 1}{N} + \frac{\eta_0}{ME_b\Omega_0} \right\}^{-1} \tag{23}$$

where $K$ denotes the number of users, $N$ is the processing gain, $\eta_0$ is the AWGN power spectral density, $E_b$ is the energy per bit and

$$q(L,\delta) = \sum_{l=0}^{L-1} \exp(l\delta) \tag{24}$$

where $\delta$ is the decay exponent of the exponential power delay profile.

The average BER, using [9], can be expressed as given in (25).

$$\overline{P}_e = \frac{1}{2\pi} \int_0^{\infty} \prod_{i=1}^{L} \left[1 + \left(\frac{t}{\eta}\right)^2\right]^{-\frac{m_l^{\,d}}{2}} \left\{ \begin{aligned} &\cos\left[\sum_{l=1}^{L} m_l^{\,d} \tan^{-1}\left(\frac{t}{\eta}\right)\right] \cdot \left[\frac{\sigma_0/2}{\sigma_0^{\,2} + t^2}\right] \cdot \left[(\sigma_0^{\,2} + t^2)^{\frac{1}{2}} + \sigma_0\right]^{-\frac{1}{2}} \\ &+ \sin\left[\sum_{l=1}^{L} m_l^{\,d} \tan^{-1}\left(\frac{t}{\eta}\right)\right] \cdot \left[\frac{1}{t} - \left[\frac{\sigma_0/2}{\sigma_0^{\,2} + t^2}\right]^{\frac{1}{2}} \cdot \left[(\sigma_0^{\,2} + t^2)^{\frac{1}{2}} - \sigma_0\right]^{-\frac{1}{2}}\right] \end{aligned} \right\} dt \tag{25}$$

Top

where, now we have

$$\nu = \frac{\bar{\Gamma}_1^{\,d}\, m_l^{\,d}}{\bar{\Gamma}_l^{\,d}}.$$

In general, the integral in (25) can be computed numerically. For example, Gaussian quadrature method of order 15 to 20 gives accurate results.

## IV. RESULTS

In DS-CDMA systems, the capacity is measured in terms of the number of users per cell or sector that can be accommodated up to a certain performance level. For voice communication purposes, the performance level is up to a raw (un-coded) average BER of 0.01. The average theoretical and simulated BER of a 2-D RAKE receiver, with a spatio-temporal diversity order 2×2 with $m_1$=2, $m_2$=1 and an inter-element spacing of 9λ /2, at an average SNR of 10dB, versus the number of users $K$ are shown in Fig. 4. The results show that 38 users can be supported up to uncoded BER of approximately .01 for δ=0

As shown in Fig. 4, the capacity of the 2-D RAKE receiver is approximately twice that of the 1-D RAKE receiver for δ= 0. The 1-D RAKE can support only 20 users. Fig 5 shows the average BER of the same 2×2 2-D RAKE receiver for inter-element spacing of 5λ/2 at 10dB and δ=0 and δ= 0.4, respectively. Comparing the results in Fig. 4 and 5, we note that reducing the spacing from 9λ /2 to 5λ /2 reduces the theoretical capacity from 38 to 35 users.

The average BER of the 1×2 1–D RAKE and the 2×2 2-D RAKE receivers for a Rayleigh (N-LOS) channel (both of the two paths are Rayleigh faded, $m_1$=$m_2$=1) is shown in Fig. 6. The corresponding average BER for a LOS channel ($m_1$=3 and $m_2$=1) is shown in Fig. 7. Comparing the two figures shows the significant difference in the spatial diversity gain between N-LOS and LOS channels. For the NLOS case, the spatial diversity increases the capacity from 10 users only for the 1-D RAKE receiver to 35 users for the 2-D RAKE receiver. For the LOS case ($m_1$=3), the spatial diversity increases the capacity from approximately 23 users for the 1-D RAKE receiver to 40 users for the 2-D RAKE receiver, which corresponds to a capacity gain factor that less than two as compared to a capacity gain factor of 3.5 for the NLOS case

## V. CONCLUSIONS

Bad urban environments are expected to generate spatio-temporal impulse responses with temporally and spatially distinct paths (each path has a distinct average delay and a distinct mean AoA).

The received paths at the BS in a wideband bad urban channel have high spatial correlations due to their small angular spread.

2-D RAKE receivers significantly outperform 1-D RAKE receivers for both single-user and multi-user cases even in LOS channels where the high spatial correlations degrade the spatial diversity gain. The capacity of 2-D RAKE receivers with a diversity order of two in both time and space was found to be as twice as the capacity of the corresponding 1-D RAKE receiver in LOS channels (with a Nakagami parameter $m$=3 for the first path) and 3.5 times the capacity of the corresponding 1-D RAKE receiver in NLOS channels.

The increase of the inter-element spacing of the ULA does not significantly improve the 2-D RAKE performance in LOS channels due to the small improvement in the spatial diversity gain.

## RERENCES


[1] A. Paulraj, B. Kalaj, and T. Kailath, " 2-D RAKE receivers for CDMA cellular systems" in Proc. *IEEE GLOBECOM*, vol 1, pp. 400-404. Dec. 1994.

[2] W. Y. C. Lee, "Effects on Correlation Between Two Mobile Radio Base Station Antennas," *IEEE Trans. on Commun*, Vol. 21, No. 11, pp. 1214-1224, November 1973.

[3] J. Salz and J. H. Winters, "Effect of Fading Correlation on Adaptive Arrays in Digital Mobile Radio," *IEEE Trans. Veh. Technol*. Vol. 43, NO. 4, pp. 1049-1057, Nov. 1994.

[4] Al-ahmadi, Saad and Asrar, U.H. Sheikh, " Spatial domain modeling of microcellular systems operating in multipath Nakagami channels". *IEEE PIMRC*, pp. 1942-1946. 2002.

[5] K. I. Pederson, P. E. Mogensen, and B. H. Fleury, "A Stochastic Model of the Temporal and Azimuthal Dispersion Seen at the Base Station in Outdoor Propagation Environments," *IEEE Trans. Veh. Technol*, Vol. 49, NO. 2, March 2000.

[6] C. Mun, C. Kang, and H. Park, "Approximation of the SNR Statistics for MRC Diversity Systems in Arbitrarily Correlated Nakagami Fading Channels," *Electronic Letters*, Vol. 35, NO. 4, pp. 266-267, Feb. 1999.

[7] S. Kotz and J. Adams, "Distributions of Sum of Identically Distributed Exponentially Correlated Gamma Variables," *Annals Math. Statist*., 35, pp. 277-283. 1964.

[8] G. P. Efthymoglou, V. A. Aalo and H. Helmken,' Performance Analysis of Coherent DS-CDMA Systems in Nakagami Fading Channel with Arbitrary Parameters,' *IEEE Trans. Veh Tech*, vol.46, no.2, May 1997.

[9] I. S. Gradshteyn and I. M. Ryzhik, *Table of Integrals, Series, and Products*. New York: Academic, 1980.


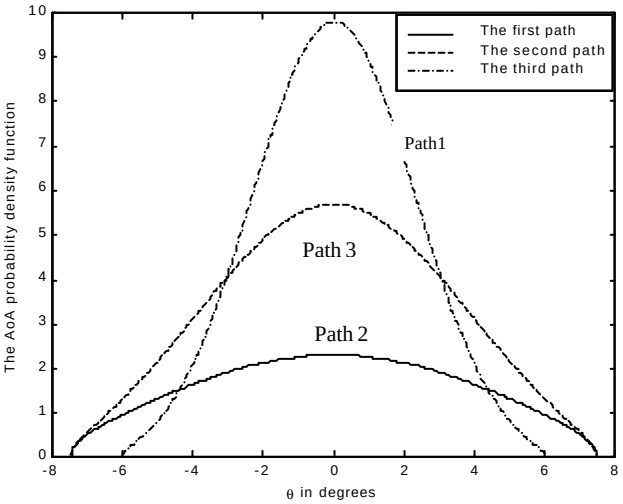


Figure 2: The AoA pdf 's of the first, second and third paths for $s_1$=30 m, $s_2$=20 m and $s_3$=15m.

Top

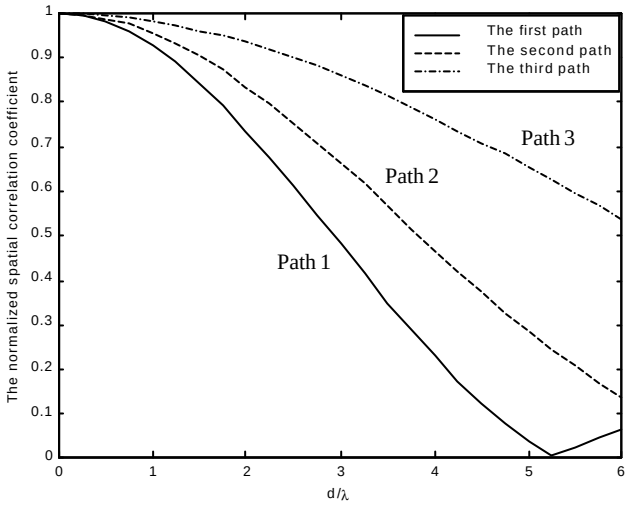


Figure 3: The spatial correlation coefficients of the three paths with $s_1$=30 m, $s_2$=20 m and $s_3$=15 m.

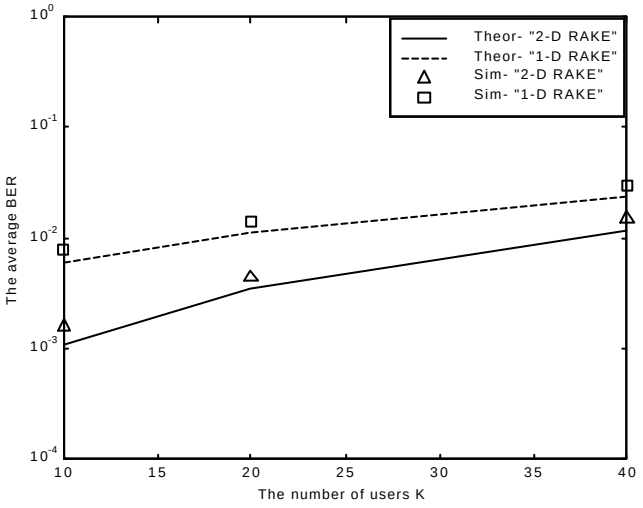


Figure 4: The average BER versus the number of users for the (1×2) 1-D RAKE and the (2×2) 2-D RAKE receivers for $m_1$=2,$m_2$=1, $d$=9λ/2 and δ=0.

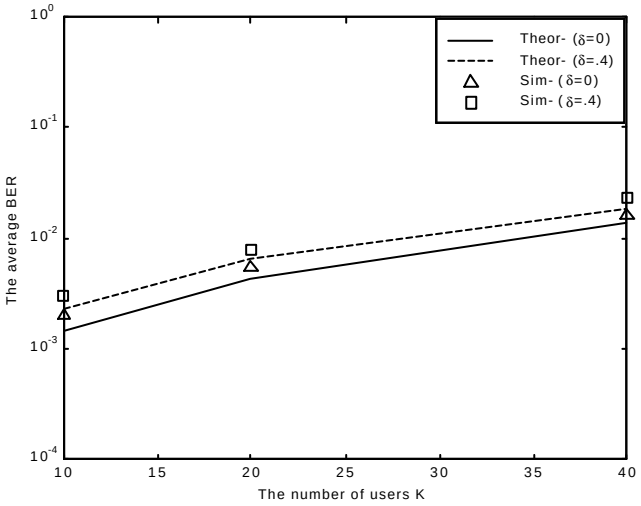


Figure 5: The average BER versus the number of users for the (2×2) 2-D RAKE receivers for $d$=5 /2 for $m_1$=2, $m_2$=1, δ=0 and δ=0.4.

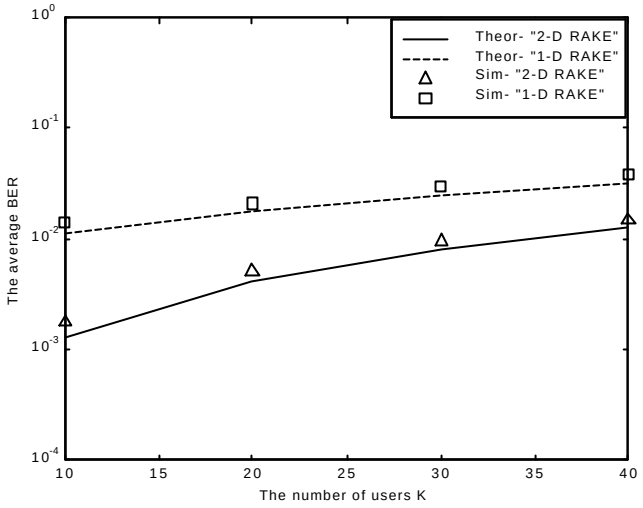


Figure 6: The average BER versus the number of users for the (1×2) 1-D RAKE and the (2×2) 2-D RAKE receivers for $d$=9λ/2, $m_1$=1 and $m_2$=1.

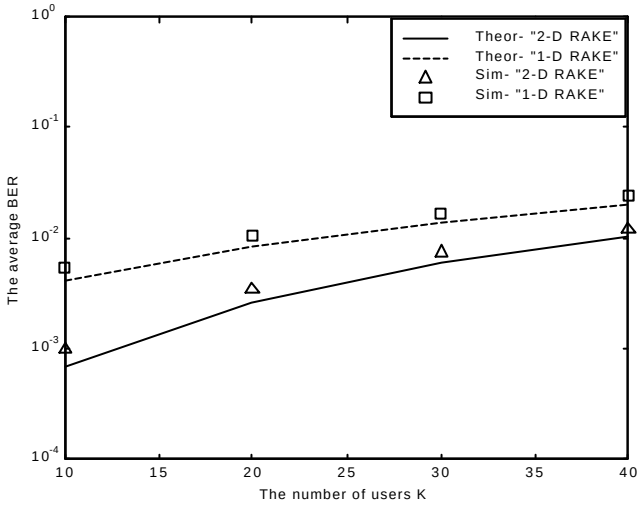


Figure 7: The average BER versus the number of users for the (1×2) 1-D RAKE and the (2×2) 2-D RAKE receivers for $d$=9λ/2 , $m_1$=3 and $m_2$=1.

Top